Desalination and Water Treatment
www.deswater.com
doi: 10.1080/19443994.2014.988660

57 (2016) 3916–3927
February

Taylor & Francis
Taylor & Francis Group

Anaerobic stabilized landfill leachate treatment using chemically activated sugarcane bagasse activated carbon: kinetic and equilibrium study

Nurshazwani Bt. Azmi, Mohammed J.K. Bashir*, Sumathi Sethupathi, Choon Aun Ng

Faculty of Engineering and Green Technology (FEGT), Department of Environmental Engineering, University Tunku Abdul Rahman, 31900 Kampar, Perak, Malaysia, Tel. +605 4688888/4559; Fax: +605 4667449; emails: shazwani103@gmail.com (N.B. Azmi), jkbashir@utar.edu.my (M.J.K. Bashir), sumathi@utar.edu.my (S. Sethupathi), ngca@utar.edu.my (C.A. Ng)

Received 28 June 2014; Accepted 11 November 2014

ABSTRACT

Adsorption via activated carbon (AC) is one of the best methods to treat stabilized landfill leachate. However, this technique has been justified due to expensive and limited resource of AC precursor. Thus, in this study, sugarcane bagasse, a cheap and abundant biomass from agricultural waste, was used to prepare AC. The prepared sugarcane bagasse activated carbon (SCAC) was tested for color, chemical oxygen demand (COD), and ammoniacal nitrogen (NH_3-N) removals from anaerobic stabilized landfill leachate. SCAC was prepared using physical and chemical activation. SCAC was characterized for its surface area, surface morphology, and functional groups. The performance of the adsorbent was examined in a batch mode study by varying the shaking speed, contact time, adsorbent dosage, and pH. The experimental results indicated that SCAC could adsorb and remove the pollutants from anaerobic municipal stabilized landfill. Removal of color, COD, and NH_3-N were favorably described by Langmuir isotherm model, with a maximum monolayer adsorption capacity of 555.56 Pt/Co, 126.58, and 14.62 mg/g, respectively. Pseudo-second-order model fits well with the experimental results and indicates that the adsorption was controlled by chemisorptions. The experimental results revealed that the optimum experimental conditions (e.g. 200 rpm shaking speed, 180 min contact time, 7 g AC dosage, and pH 7) resulted in 94.74, 83.61, and 46.65% removal of color, COD, and NH_3-N, respectively.

Keywords: Anaerobic landfill; Leachate treatment; Sugarcane waste; Adsorption isotherm; Kinetics

1. Introduction

Landfill leachate is a dark color liquid with a strong smell generated from excess water percolates with the heterogeneous mixture of organic and inorganic loads deposited within the waste layers in the landfill [1]. The formation of landfill leachate involves a complex interplay between hydrological and biogeochemical reactions that acts as a mass transfer process for producing sufficiently high moisture content within landfill in order to start the liquid flow, and it is induced by gravity force, precipitation, irrigation, surface runoff, snowmelt, recirculation, liquid waste co-disposal, refuse decomposition, groundwater intrusion, and initial moisture content present within the landfill [2]. As a consequence, landfill leachate contains high concentration of biodegradable and

*Corresponding author.

non-biodegradable organic compounds, ammonia nitrogen, heavy metals, and chlorinated organic and inorganic salts [3]. The quantity and quality of leachate is influenced by a number of factors (seasonal precipitation and waste composition), but it is mainly indicated by the landfill age [4]. Stabilized leachate generated from old landfill basically contains high concentration of ammoniacal nitrogen (NH_3-N), high proportion of non-biodegradable compounds (humic and fulvic acid) with low COD: BOD_5 ratio [3] compared to leachate generated from young landfill. As a consequence, biological treatment methods, such as activated sludge, anaerobic filtration, and anaerobic lagoons, which normally effect reducing concentrations of organic matter in young landfill leachate [5] are ineffective for treating stabilized leachate. Thus, physico-chemical techniques are demanded for stabilized landfill leachate treatment [6–9]. Several physico-chemical treatments have been studied for stabilized landfill leachate treatments including electro-oxidation [10,11], ion-exchange [11,12], coagulation–flocculation [13,14], and adsorption [15].

However, economic inconvenience limits the utilization of most physico-chemical processes in treating stabilized landfill leachate including adsorption. Adsorption has been reported to have several advantages compared to other physico-chemical techniques. These includes the simplicity of design, low quantity of residue, low initial cost, ease of recovery, and possibility to reuse the adsorbent [16]. Recently, utilization of nanoparticles in wastewater treatment have received special attention by several researchers [17,18]. For example, utilization of iron oxide nanomaterials has received much attention due to their unique properties, such as extremely small size, high surface-area-to-volume ratio, surface modifiability, excellent magnetic properties, and great biocompatibility [18]. Feitoza et al. [18] reported that nanoparticles showed high capability in heavy metal ion uptake [17]. It was indicated that these nanoadsorbents can be used as highly efficient separable and reusable materials for removal of toxic metal ions [18]. Meanwhile, another superior adsorption approach is activated carbon (AC) adsorption. Adsorption via AC has been reported as an effective method for removing high molecular weight refractory organic compounds from landfill leachate [15]. A number of unique characteristics such as high adsorption capacity, microporous structure, extended surface area, high degree of surface reactivity [16], thermostability, low acid/base reactivity, and removal ability for a broad range pollutants makes AC as one of the best filtration media in the world. However, the major limitations of AC utilization in leachate treatment process are owing to the high production cost and expensive carbonaceous materials.

Recently, researchers are focusing on agriculture waste as a potential carbonaceous material in AC production for wastewater treatment. Thus, the present study aims to examine the potential of sugarcane bagasse activated carbon (SCAC) as a renewable source of AC to treat leachate generated from mature anaerobic landfill. The effectiveness of the treatment process variables (e.g. shaking speed, contact time, dosage, and pH) was investigated. Besides, the adsorption isotherms and kinetics were evaluated to explain color, COD, and NH_3-N adsorption via SCAC.

2. Materials and methods

2.1. Site description

Sahom landfill is an anaerobic landfill located in Kampar, Perak, Malaysia. It is being operated since year 1992 in a land area of 37 acres. Although the landfill is equipped with leachate collection system, there is no leachate treatment system prior to discharge to the nearby lake. Sahom landfill is mainly used for handling municipal waste collected from Kampar district. In 2010, the population of the service was 101,183 capita with a total daily MSW collected amount of 100 tonnes.

2.2. Leachate sampling and characterization

The leachate samples were collected from leachate collection pond and instantaneously transported to the laboratory, and stored in darkness at 4°C with minimum exposure to surrounding air in order to minimize the chemical and biological changes. The characteristics of leachate samples were analyzed according to standard methods of water and wastewater [19]. The characteristics of Sahom landfill samples are presented in Table 1. The color concentration was measured at 455 nm wavelength using Hach color method 8,025, whereas COD concentration was measured using Hach DR 6000 spectrophotometer at 620 nm wavelength. Closed reflux colorimetric method was used to determine COD. In addition, NH_3-N was measured using 4500-NH_3 Phenate Method (*F*) with spectrophotometer DR 6000 at 640 nm wavelength. The method involves addition of phenol solution together with hypochlorite and nitroprusside catalyst to the sample. Ammonia reacts to form indophenol, which has an intense blue color. Heavy metals were measured using inductively coupled plasma mass spectrometry (ICP-MS) (model NexION 300Q Perkin Elmer ICP-MS, USA). All tests were conducted in accordance with the standard methods for examination of water and wastewater [19].

Table 1
Sahom landfill leachate characteristics

Parameters	Unit	Concentration
Temperature	°C	26.9–27.1
pH	–	8.60–8.75
Conductivity	ms	10.93–11.02
Resistivity	Ω	90.04–90.08
Turbidity	ntu	105.6–126.0
Color	Pt/Co	3,300–3,500
COD	mg/L	1,490–1,570
NH_3-N	mg/L	1,860–1,950
BOD_5	mg/L	106–120
BOD_5/COD	–	0.071–0.076
Total Suspended Solids	mg/L	203–227
Total iron	mg/L	7.2850
Copper	mg/L	0.0853
Zinc	mg/L	2.4570
Cadmium	mg/L	0.0147
Lead	mg/L	0.2196
Chromium	mg/L	0.0853
Manganese	mg/L	25.470

2.3. Preparation of AC

In this experiment, SB was used as the precursor for AC production. SB was collected from neighboring stall in Kampar, Perak, Malaysia. The raw precursors were cut into small pieces, boiled, and washed exhaustively in order to remove adhering impurities from the surface. The SB was dried in an oven at 105 °C overnight to remove unwanted moisture. The dried bagasse was ground with 0.1 mm blade using grinding machine (ZM200, Germany) and sieved by mechanical sieve shaker (R30050, Malaysia) to retain particle sizes ranging from 1.4 to 0.5 mm. The carbonization process was performed in muffle furnace at 700 °C for 2 h under inert atmosphere. The char produced was mixed with potassium hydroxide (KOH) solution with impregnation ratio (Char: KOH) at 1:2.7 wt.% which was selected based on preliminary experiments. The wet bagasse was dried at 105 °C for three days before carbonization in muffle furnace within 3 h at 600 °C with a ramping rate at 10 °C/min [20]. In order to remove organic matter residues and alkalis, the resultant AC was washed with 0.1 M HCI and rinsed, repetitively with deionized water until the pH of the filtrate reach around 6.5–7.0. Finally, the prepared AC was dried for 24 h prior to leachate treatment process.

2.4. Batch study

The batch adsorption experiments were conducted in a series of 250 ml Erlenmeyer flask containing mixture of 100 ml of raw leachate with SCAC. The flasks were capped and agitated in an orbital shaker under specific experimental conditions. The optimization studies were done by one-variable-at-a-time method by monitoring the influences of one factor at a time of an experiment, where only one factor is varied and others remained constant [21]. The adsorptive uptake efficiencies of color, COD, and NH_3-N were investigated by testing the influence of operational variables including shaking speed, contact time, AC dosage, and pH. After each run, the media were filtered and the filtrates were kept for analysis of pollutants removal.

2.5. Equilibrium studies

In this study, adsorption isotherm models were used to describe the performance of the media and the relationship between the adsorbent AC and the dissolved adsorbates (pollutants) in the solution. According to Droste [22], adsorption isotherm describes the relationship between the concentration of adsorbate that accumulates on the adsorbent and equilibrium concentration of the dissolved adsorbate. The amounts of adsorbate accumulated on the adsorbent were measured by the difference between the initial concentration of adsorbate with the concentration of adsorbate at equilibrium within the dissolved solution where it is expressed by following equation:

$$q_e = \frac{(C_0 - C_e)V}{m} \quad (1)$$

where q_e is the amount of adsorption at equilibrium, C_0 is the initial concentration for the adsorbate, while C_e is the amount of adsorbate at equilibrium in the form of color (Pt/Co/L), COD (mg/L), and NH_3-N (mg/L), V (L) is the volume of the solution, and m(g) is the mass of the dry sorbent used.

The percentage of pollutant removal is calculated as follows:

$$\text{Removal percentage} = \frac{(C_0 - C_e)}{C_0} \times 100 \quad (2)$$

where C_0 and C_e are the initial and equilibrium stage liquid-phase concentrations of the adsorbate in terms of color, COD, and NH_3-N .

3. Result and discussion

3.1. Leachate characteristic

Table 1 shows the characteristics of leachate generated from Sahom landfill located in Perak, Malaysia.

The leachate has high amount of color (8,960 Pt/Co), COD (2,740 mg/L), and NH_3-N (2,113 mg/L), with low BOD_5:COD ratio. As BOD_5:COD ratio is less than 0.1, Sahom landfill leachate is classified as stabilized leachate [23]. According to Huo et al., most of the organic materials present in stabilized leachate contain refractory compounds such as humic- and fulvic-like fractions which are not biodegradable [24]. As a consequence, the effectiveness of biological process decreases and physico-chemical processes, particular adsorption, may become one of the appropriate options.

3.2. SCAC characterization

The pore structural characteristic, Fourier transform infrared spectrometer (FTIR) analysis, and scanning electron microscope (SEM) images were carried out to study the characteristics of SCAC.

3.2.1. Pore structural analysis

Table 2 summarizes the pore structural characteristic in terms of BET surface area, external surface area, Langmuir surface area, and micropore volume of SCAC before and after activation. Based on the N_2 adsorption isotherm, the BET surface area was greatly improved from 6.3875 to 99.9487 m^2/g. The same goes to external surface area (from 10.0164 to 43.5137 m^2/g), Langmuir surface area (from 7.684 to 111.7860 m^2/g), and micropore volume (from 0.001580 cm^2/g to 0.023061 m^2/g), respectively. These results indicate that the sugarcane bagasse is an efficient precursor for AC production.

3.2.2. FTIR spectra analysis

The functional groups on the surface of SCAC were identified by FTIR analysis in the scanning range of 4,000–400 cm^{-1} by FTIR spectrophotometer. Sugarcane is a lignocellulosic compound and it is generally considered as structures built by cellulose molecules, organized in micro fibrils and surrounded by hemicellulosic materials, lignin and pectin along with small amounts of protein [25]. The FTIR spectra of SCAC and sugarcane husk are presented in Fig. 1. The spectrum revealed diagnostic band at 3,426/3,434 cm^{-1} represents O–H group and stretching around 1,384/1,383 cm^{-1} illustrates the presence of C–H deformation [26]. These bands might be attributed to the cellulose and hemicellulose contents in SC husk, confirming the appearance of lignocellulosic matrix in this biomass [27]. The presence of strong C–O band at 1,052 is due to $–OCH_3$ groups in addition to the peaks at 605/cm related to bending modes of aromatic compounds confirming the presence of lignin structure-incorporated sugarcane bagasse [28]. Moreover, a weak intensity band located at 1,637/cm was argued to stretching vibration of carboxylic acid of galacturonic acid [29].

In SCAC, the functional group at 1,637 cm^{-1} disappears while the skeletal C–C vibrations in aromatic ring (1,562 cm^{-1}) are intensified. This can be attributed to the decrease in the oxygen groups such as ether and alcohol by the heat treatment process of pyrolysis which indicates that the functional groups are thermally unstable [30]. In addition, the appearance of 2,373 cm^{-1} band of alkynes (C≡C) groups in SCAC may be due to the release of light volatile matter such as hydrogen, resulting from the heat treatment process in the char production [31].

After adsorption treatment (Fig. 1(c)), it was found that, oxygen containing functional groups like –OH groups are affected after uptake process. This is judged from shifts in its position to lower frequency, shape, or band intensity from 3,426 to 3,423 cm^{-1}. The results indicated that the participation of these groups via oxygen for pollutant binding in leachate to SCAC is in agreement with person principal for hard–soft acids and bases [32].

3.2.3. SEM analysis

SEM graphs for the char and SCAC are presented in Fig. 2. Fig. 2(a) shows the pore structure of sugarcane bagasse husk prepared during pyrolysis process with the development of rudimentary pore structure on char fraction. According to Mohamed et al., during pyrolysis process, non-carbon elements such as hydrogen, oxygen, and nitrogen released in the form of tars and gases leaving a rigid carbon skeleton with a rudimentary pore structure formed from the aromatic compounds [33]. Consequently, activation by physico-chemical process enhanced the pore structure of sugarcane-derived AC. Pretreatment of the char with dehydrating agent (KOH) inhibits formation of tar and other undesired products [33], and at the same time

Table 2
Pore structural characteristic of SCAC

Properties	Char	SCAC
BET surface area (m^2/g)	6.3875	99.9487
External surface area (m^2/g)	10.0164	43.5137
Langmuir surface area (m^2/g)	7.6884	111.7860
Micropore volume (cm^3/g)	0.001580	0.023061

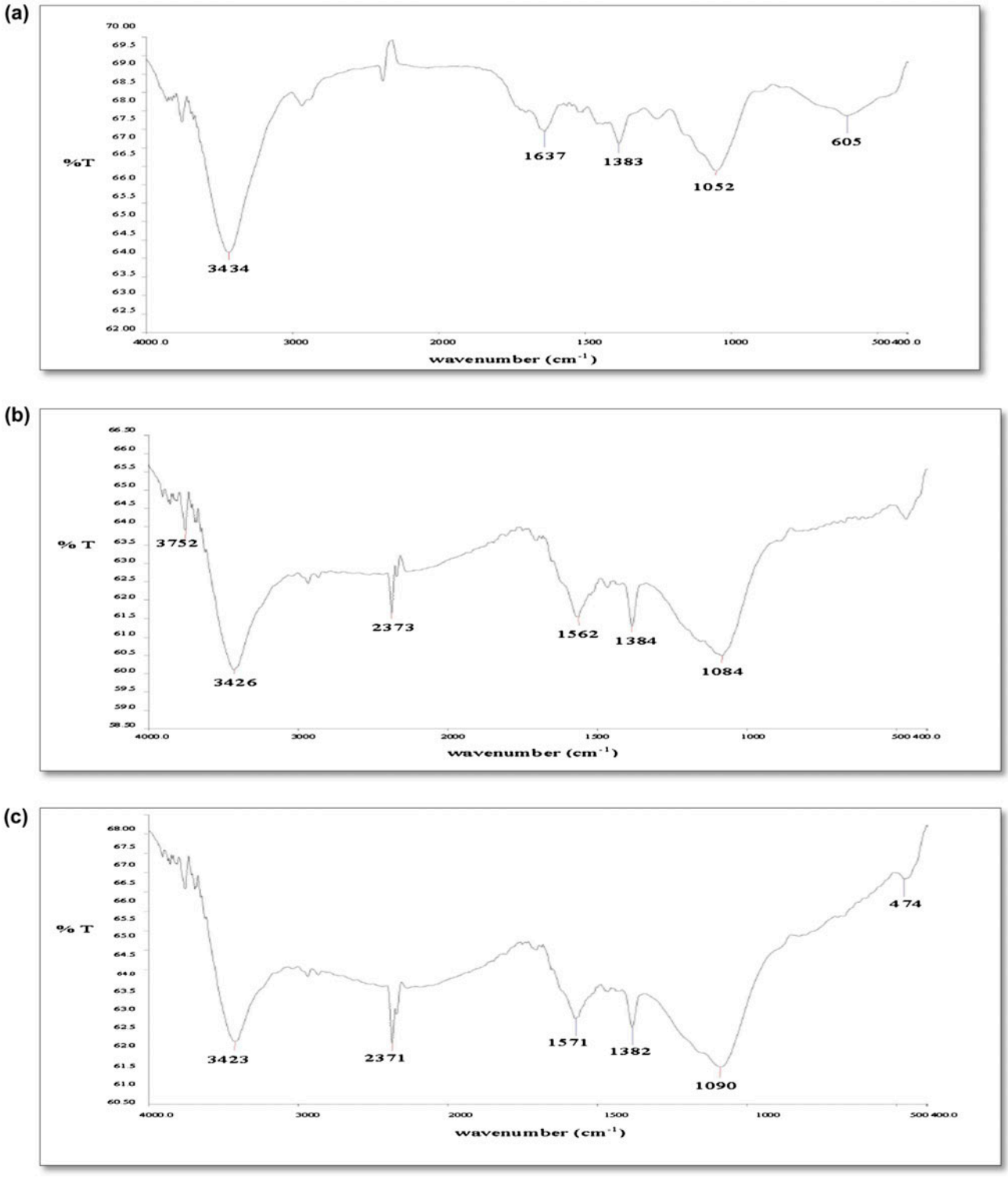

Fig. 1. FTIR analysis of (a) Sugarcane husk, (b) SCAC before treatment, and (c) SCAC after treatment.

generates porosity by carbon oxidation and hydroxide reduction [34]. Consequently, CO_2 creates AC with larger micropore volume and narrower micropore size distribution leading to higher adsorption capacity [33].

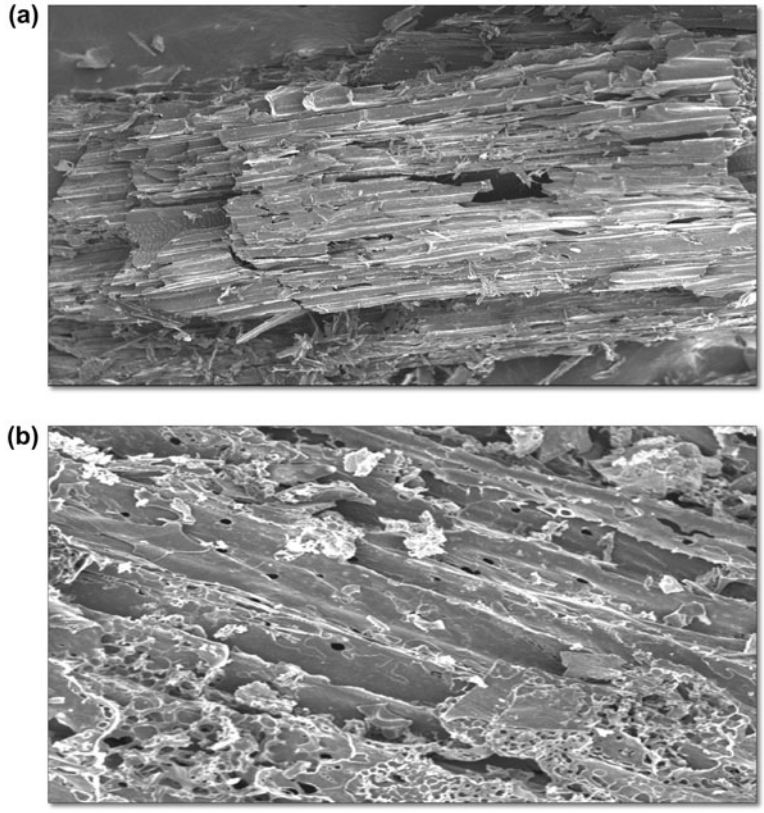

Fig. 2. SEM micrograph of (a) char at 200× magnification and (b) SCAC at 900× magnification.

3.3. Optimization of adsorption process

3.3.1. Shaking speed

The effects of shaking speed on the removal efficiency of color, COD, and NH_3-N were illustrated in Fig. 3. The effects were studied using 2 g of AC with varied shaking speed (0–300 rpm) within 180 min shaking time. Based on Fig. 3, percentage removal increased with increasing shaking speed, and becomes constant after 200 rpm. The optimum percentage removal for color (82.9%), COD (72.9%), and NH_3-N (31.4%) was obtained at 200 rpm. According to Chabani et al. [35], the resistance of boundary layer surrounding the adsorbates deteriorates at strong agitation rates. Thus, the adsorption rate becomes faster at higher shaking speed.

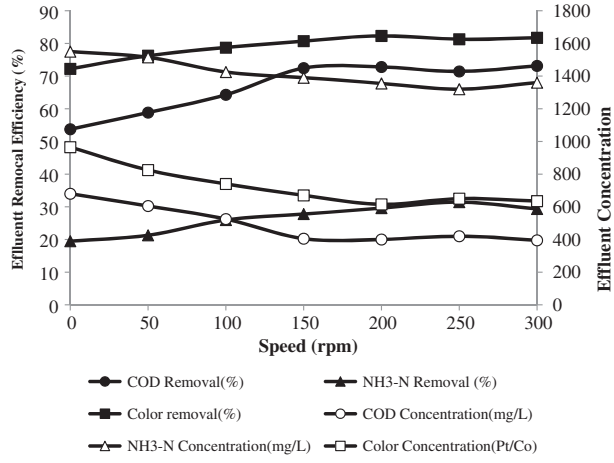

Fig. 3. The effluent removal (%) and effluent concentration of COD, NH_3-N, and Color at different shaking speed (rpm).

3.3.2. Contact time

The effects of contact time on percentage removals of color, COD, and NH_3-N were illustrated in Fig. 4. The AC dosage (2 g) and shaking speed (200 rpm) were remained constant with varied contact time (10–360 min) throughout the experiment. Based on Fig. 4, percentage removal of pollutants (color, COD, and NH_3-N) increased with longer period of contact time. The optimum contact time was 180 min with percentage removal of color at 80%, COD at 72.98%, NH_3-N

at 33.06%, and decreased when it is further increased beyond it. In the early stage, there are larger surface sites that lead to higher adsorption capacity at a short period of time. However, as the contact time prolonged and approached to equilibrium, the availability of sorption sites decrease and becomes difficult to occupy due to repulsive forces between the solute molecules on the solid and bulk phases. As a consequence, the removal rates slow down due to the competition for the adsorption sites [36].

3.3.3. Dosage

The effect of SCAC dosage on percentage removal of color, COD, and NH_3-N was illustrated in Fig. 5. The shaking speed (200 rpm) and contact time (180 min) remained constant with varied SCAC dosages (0–9 g) throughout the experiments. Based on Fig. 5, it is apparent that adsorptive removal of color, COD, and NH_3-N increased by increasing adsorbent dosage from 0 to 9 g. However, adsorbent dosage presents a profound effect on the adsorption process due to the reason that it predicts the cost of adsorbent per unit of pollutant to be treated [37]. Thus, the optimum AC dosage was 7 g/100 ml with removal efficiency of 94.74 color, 83.61 COD, and 46.65 NH_3-N, respectively.

3.3.4. pH

The adsorptive behavior of SCAC on color, COD, and NH_3-N removal is illustrated in Fig. 6. Based on Fig. 6, increasing solution pH from 3 to 11 showed steady increase in adsorptive uptake of color from 78.55 to 84.06% and COD from 71.62 to 76.35%, meanwhile, percentage removal of NH_3-N showed an

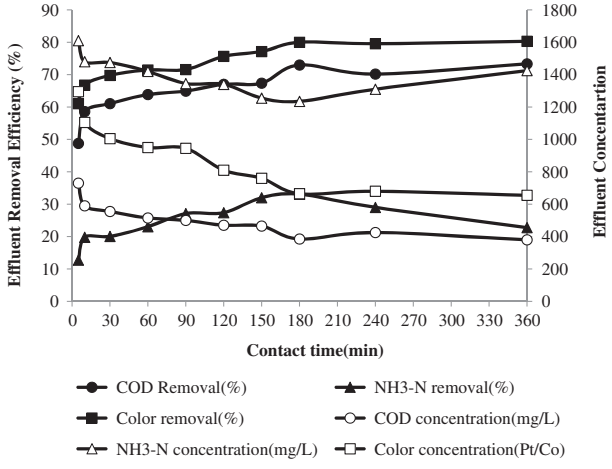

Fig. 4. The effluent removal (%) and effluent concentration of COD, NH_3-N, and color at different contact time (min).

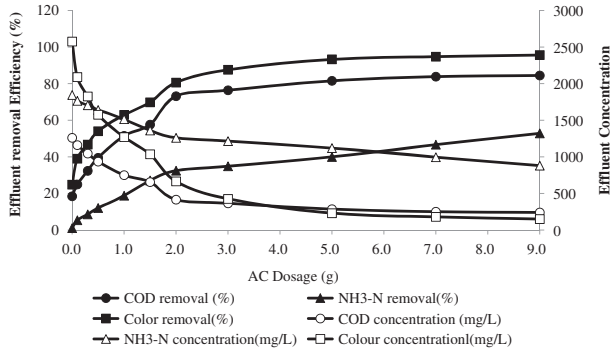

Fig. 5. The effluent removal (%) and effluent concentration of COD, NH_3-N, and color at different AC dosage (g).

enhancement from 15.69 (pH 3) to 63.3% (pH 11). This may be because, the adsorbents were highly selective for H_3O^+ when the concentration of H_3O^+ was high at low pH [38]. Thus, at low pH, H_3O^+ competed with NH_3^+ for exchange sites in adsorbent. The same result was found in removal of iron by coffee ground AC [38]. According to Wu et al. [39], pH of the solution played an important role in enhancing pollutants removal efficiency as it influences the adsorbent surface charge as well as degree of ionization of adsorbates present in the solution.

3.4. Isotherm analysis

The adsorption characteristics in this study were analyzed using the Langmuir and Freundlich isotherm models which are the most common models for describing the adsorption properties of adsorbents used in water and wastewater treatment [35].

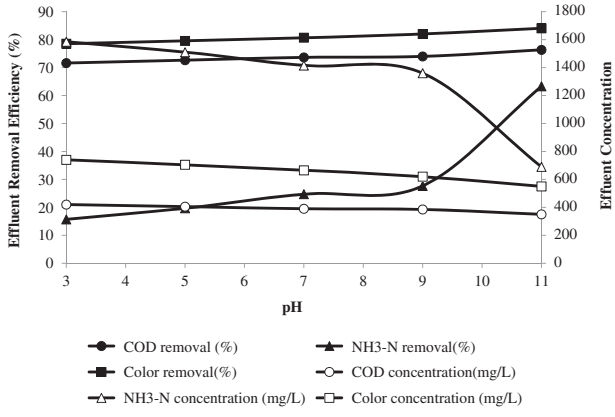

Fig. 6. The effluent removal efficiency (%) and effluent concentration of COD, NH_3-N, and color at different pH.

The Langmuir isotherm model assumes monolayer coverage of adsorbate over a homogenous adsorbent surface. The basic assumption is that sorption takes places at specific homogenous site of adsorbent.

The Langmuir isotherm is as follows:

$$\frac{1}{q_e} = \frac{1}{QbC_e} + \frac{1}{Q} \tag{3}$$

where C_e is the equilibrium liquid-phase concentration, q_e is the equilibrium uptake capacity (mg/g), while Q (mg/g) and b (L/mg) are the Langmuir constants. A straight line was obtained when $1/q_e$ was plotted against $1/C_e$. Q was evaluated from the slope, whereas b was determined from the intercept as demonstrated in Fig. 7. The equilibrium data were fitted to the Langmuir isotherm model. The constants, together with the R^2 value are listed in Table 3. As shown in Table 3, the adsorption capacities for color, COD, and NH_3-N were 555.56 Pt-Co/g, 126.58 mg/g, and 14.62 mg/g, respectively. The characteristic of the Langmuir isotherm can be expressed using the equilibrium parameter, R_L [40].

$$R_L = \frac{1}{(1 + b\ C_0)} \tag{4}$$

where b is Langmuir constant, and C_0 is the initial pollutant concentration (mg/L). The value of R_L indicates whether the isotherm is unfavorable ($R_L > 1$), linear ($R_L = 1$), favorable ($0 < R_L < 1$), or irreversible ($R_L = 0$).

Meanwhile, Freundlich isotherm theory assumes multilayer coverage of adsorbate over a heterogenous adsorbent surface. The Freundlich isotherm is expressed as follows:

$$\log q_e = \log K + \frac{1}{n}\log C_e \tag{5}$$

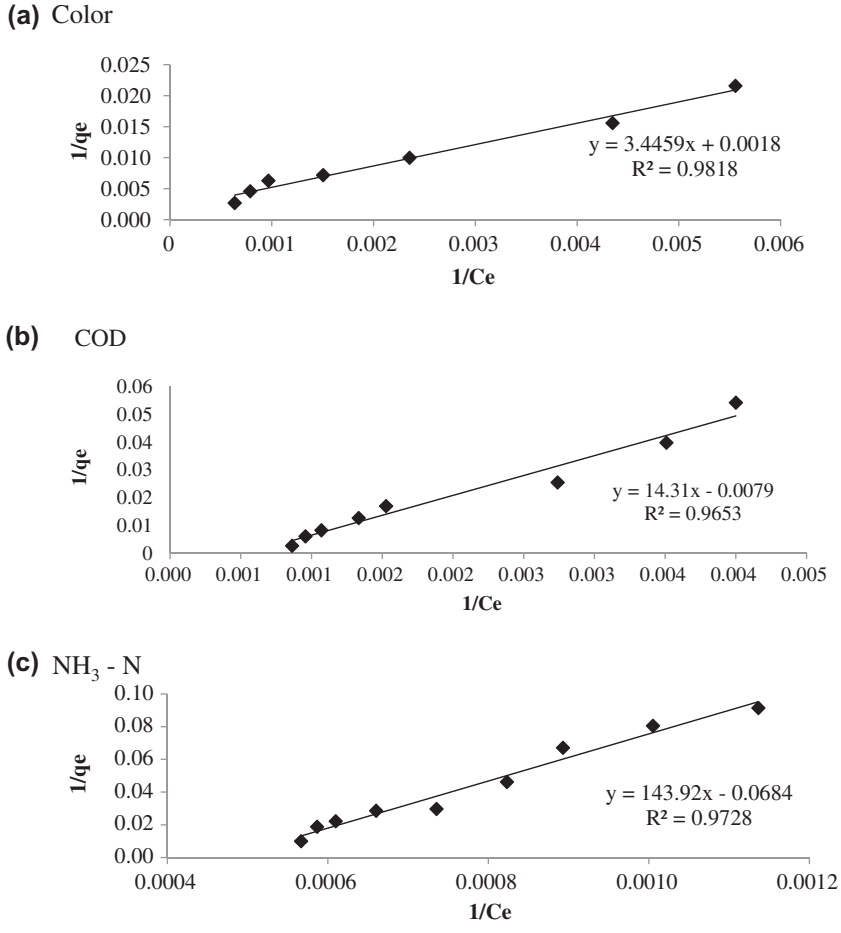

Fig. 7. Langmuir isotherm for adsorptive removal of (a) color, (b) COD, and (c) NH_3-N.

Table 3
Isotherm equation parameters for color, COD, and NH_3-N adsorption using SCAC

Parameter	Langmuir isotherm coefficient			Freundlich isotherm coefficient		
	Q (mg/g)	b (L/mg)	R^2	K (mg/g), ((L/mg)1/n)	$1/n$	R^2
Color	555.556	0.0005224	0.9818	0.678734617	0.8199	0.9524
COD	126.582	0.0005521	0.9653	0.002761849	1.5929	0.9085
NH_3-N	14.6199	0.0004753	0.9728	0.000000037	2.847	0.923

where C_e is the equilibrium liquid-phase concentration of pollutant, q_e is the equilibrium uptake capacity (mg/g), K is the indicator of the adsorption capacity in mg/g (L/mg), and $1/n$ is the constant indicator of the intensity of the adsorption. The slope of $1/n$ is ranging between 0 and 1, where it indicates higher surface heterogeneity as the value close to zero. The plot of log q_e vs. log C_e gives a straight line with slope $1/n$. The K value was obtained by the intercept value as shown in Fig. 8.

Table 3 shows the K value, $1/n$, and the linear regression correlation (R^2) for color, COD, and NH_3-N, respectively, based on Freundlich model. Referring to the Table 3, $1/n$ value of color, COD, and NH_3-N were 0.82, 1.89, and 2.85, respectively. A value of $1/n < 1$ indicates a normal Langmuir isotherm, whereas

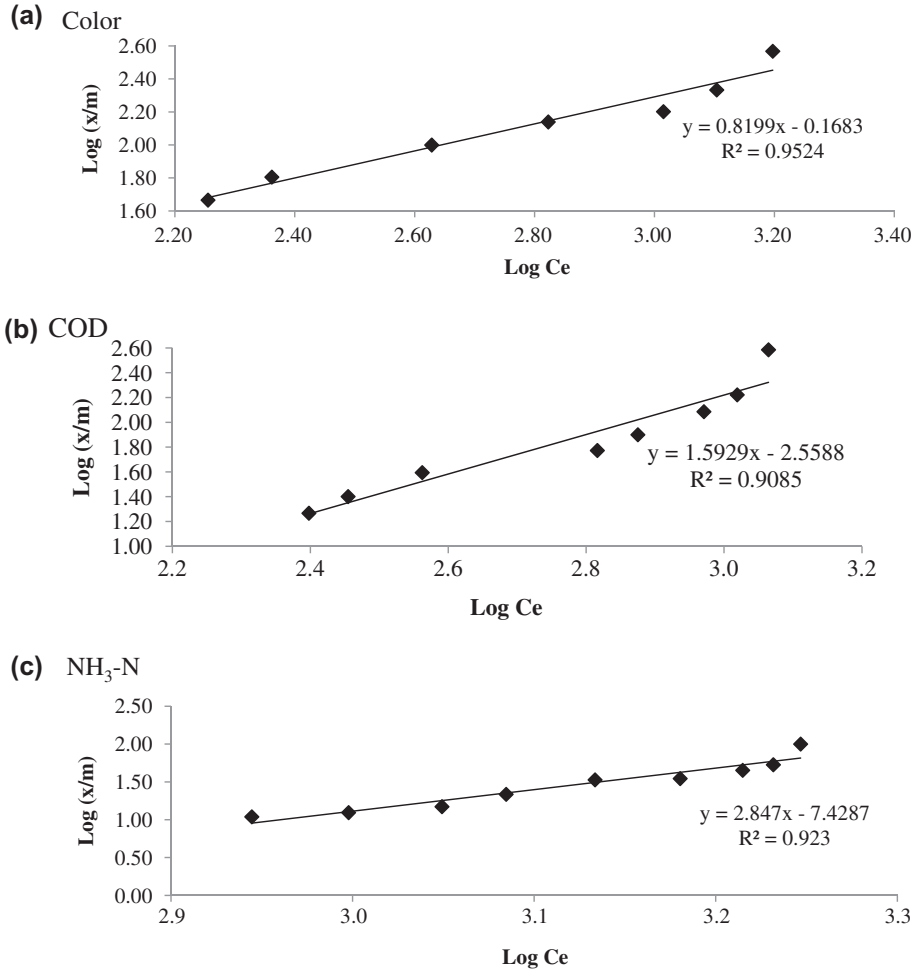

Fig. 8. Freundlich isotherm for adsorptive removal of (a) color, (b) COD, and (c) NH_3-N.

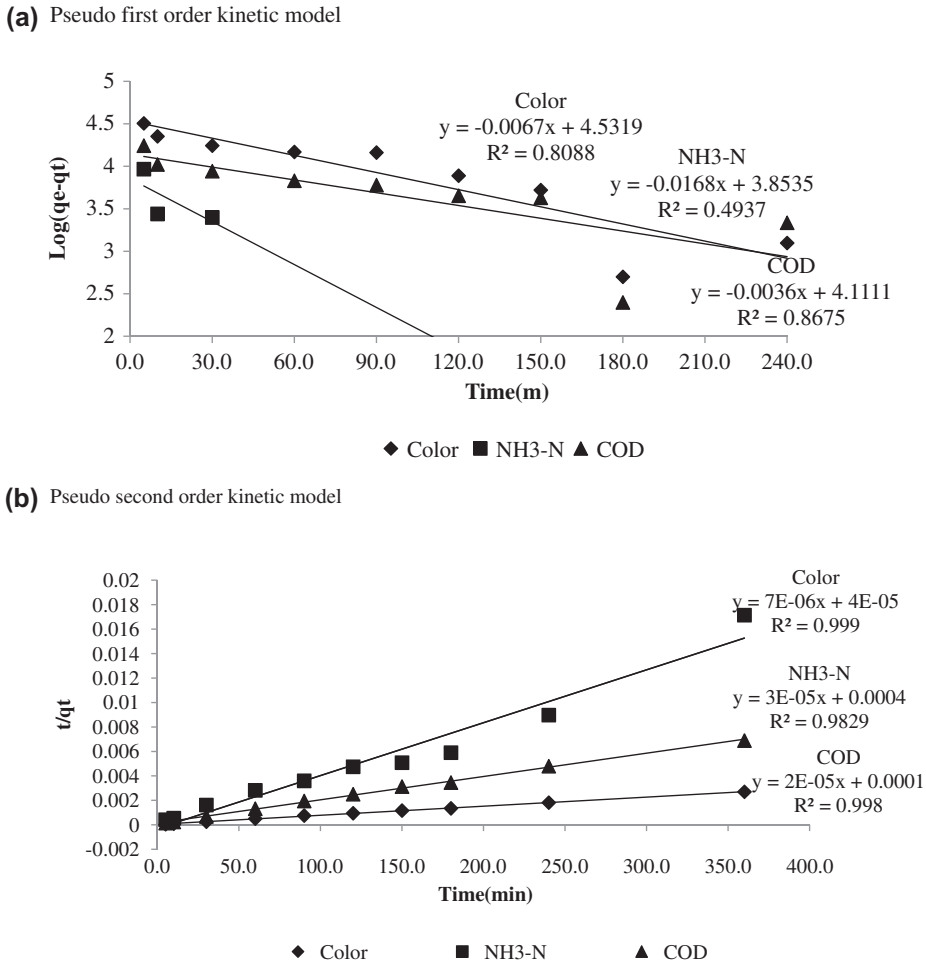

Fig. 9. (a) Pseudo-first-order kinetic model (b) Pseudo-second-order kinetic model for color, COD, and NH_3-N adsorption on SCAC.

Table 4
Kinetic model parameters for color, COD, and NH_3-N adsorption by SCAC

	Pseudo-first-order model			Pseudo-second-order model		
Parameter	K_1 min^{-1}	$q_{e,\ cal}$ (μg/g)	R^2	K_2 (g/μg min)	$q_{e,\ cal}$ (μg)	R^2
Color	0.0154	34,032.98	0.8088	8.17×10^{-7}	142,857	0.9975
COD	0.0115	13,753.08	0.5702	4.00×10^{-6}	50,000	0.9983
NH_3-N	0.0159	19,760.59	0.8454	5.33×10^{-6}	25,000	0.9570

$1/n > 1$ is indicative for cooperative adsorption [41]. The adsorption of color, COD, and NH_3-N is rationally explained by Langmuir and Freundlich isotherm models. However, the Langmuir model yielded the best fit, as the R^2 values were relatively high; color (0.9818), COD (0.9653), and NH_3-N (0.9728) compared to Freundlich model; color (0.9524), COD (0.9085), and NH_3-N (0.9230).

3.5. Adsorption kinetics

The experimental efficiency is controlled by the kinetics adsorption. Kinetic modeling was normally used to investigate the mechanism of adsorption and the potential rate controlling the process such as mass transfer and chemical reaction [12]. In this study, the adsorption kinetics of color, COD, and NH_3-N was investigated. Several kinetic models are available for

adsorption process and the most commonly used kinetic models are pseudo-first-order and pseudo-second-order models [35].

The pseudo-first-order model is illustrated as follows:

$$\log(q_e - q_t) = \log(q_e) - \frac{k_1 t}{2.303} \quad (6)$$

The pseudo-second-order model is expressed as follows:

$$\frac{t}{q_t} = \frac{1}{k_2 q_e^2} + \frac{t}{q_e} \quad (7)$$

where q_t and q_e are the amounts of pollutants adsorbed at time (t) and equilibrium which are color (Pt/Co), COD (mg/L), and NH_3-N (mg/L), and k_1, k_2 (g/mg min) are the equilibrium rate constants of the pseudo-first-order and pseudo-second-order models, respectively.

Fig. 9 shows the correlation coefficient (R^2) for both models, where pseudo-second-order kinetic model has high R^2 value compared to pseudo-first-order kinetic model, and the calculated equilibrium sorption capacities (q_e) also agreed well with experimental data as presented in Table 4. Adsorption reaction by the pseudo-second-order model indicates that the sorption process of pollutant was controlled by chemisorptions [40]. As pseudo-second-order model was more favorable compared to pseudo-first-order model, it shows that the adsorption process for color, COD, and NH_3-N was controlled by chemisorptions.

4. Conclusion

This research investigated the effectiveness of AC prepared from sugarcane bagasse as a low cost and abundant biomass for stabilized landfill leachate treatment. The batch study was designed with varied experimental conditions in terms of shaking speed, contact time, AC dosage, and pH. The adsorptive removals of color, COD, and NH_3-N were studied using isotherm and kinetic models. Based on the experiment result, the adsorptive removal of color, COD, and NH_3-N onto SCAC favorably fitted with Langmuir isotherm with a maximum monolayer adsorption capacity for color, COD, and NH_3-N were 555.56 Pt-Co/g, 126.58, and 14.62 mg/g, respectively. Meanwhile, pseudo-second-order model predicts the best kinetic adsorption models with high R^2 value compared to pseudo-first-order model which indicates that the adsorption process was controlled by chemisorptions. Shaking speed, contact time, and adsorbent dosage are the critical parameters affecting the adsorption of SCAC with the greatest adsorptive removal at 94.74% (color), 83.61% (COD), and 46.65% (NH_3-N), respectively.

Acknowledgments

The authors wish to acknowledge the Universiti Tunku Abdul Rahman (UTAR) for its financial support under the UTARRF scheme (No. UTARRF/2012-C2/M03 & UTARRF/2013-C2/L12).

References

[1] P. Yao, Perspectives on technology for landfill leachate treatment, Arabian J. Chem. (in press), doi: 10.1016/j.arabjc.2013.09.031.
[2] K.Y. Foo, B.H. Hameed, A short review of activated carbon assisted electrosorption process: An overview, current stage and future prospects, J. Hazard. Mater. 170 (2009) 552–559.
[3] S. Renou, J.G. Givaudan, S. Poulain, F. Dirassouyan, P. Moulin, Landfill leachate treatment: Review and opportunity, J. Hazard. Mater. 150 (2008) 468–493.
[4] M.J.K. Bashir, H.A. Aziz, M.S. Yusoff, M.N. Adlan, Application of response surface methodology (RSM) for optimization of ammonical nitrogen removal from semi-aerobic landfill leachate using ion exchange resin, Desalination 254 (2010) 154–161.
[5] A.D. Borgi, A.D. Binaghi, A. Converti, M.D. Borgi, Combined treatment of leachate and municipal wastewater by activated sludge, CABEQ. 17 (2003) 277–283.
[6] S.S. Abu Amr, H.A. Aziz, M.N. Adlan, M.J.K. Bashir, Pretreatment of stabilized leachate using ozone/persulfate oxidation process, Chem. Eng. J. 221 (2013) 492–499.
[7] S.S. Abu Amr, H.A. Aziz, M.N. Adlan, M.J.K. Bashir, Optimization of semi-aerobic stabilized leachate treatment using ozone/Fenton's reagent in the advanced oxidation process, J. Environ. Sci. Health. Part A. 48 (2013) 720–729.
[8] M.J.K. Bashir, H.A. Aziz, S.Q. Aziz, S.S. Abu Amr, An overview of electro-oxidation processes performance in stabilized landfill leachate treatment, Desalin. Water Treat. 51 (2013) 2170–2184.
[9] M.J.K. Bashir, H.A. Aziz, S.S. Abu Amr, S. Sethupathi, C.A Ng, J.W Lim, The competency of various applied strategies in treating tropical municipal landfill leachate, Desalin. Water Treat. (in press), doi: 10.1080/19443994.2014.901189.
[10] M.J.K. Bashir, M.H. Isa, S.R.M. Kutty, Z.B. Awang, H.A. Aziz, S. Mohajeri, I.H. Farooqi, Landfill leachate treatment by electrochemical oxidation, Waste Manage. 29 (2009) 2534–2541.
[11] M.J.K. Bashir, H.A. Aziz, M.S. Yusoff, New sequential treatment for mature landfill leachate by cationic/anionic and anionic/cationic processes: Optimization and comparative study, J. Hazard. Mater. 186 (2011) 92–102.

[12] M.J.K. Bashir, H.A. Aziz, M.S. Yusoff, S.Q. Aziz, Color and chemical oxygen demand removal from mature semi-aerobic landfill leachate using anion-exchange resin: An equilibrium and kinetic study, Environ. Eng. Sci. 29 (2012) 297–305.
[13] W. Li, T. Hua, Q. Zhou, S. Zhang, F. Li, Treatment of stabilized landfill leachate by the combined process of coagulation/flocculation and powder activated carbon adsorption, Desalination 264 (2010) 56–62.
[14] S. Ghafari, H.A. Aziz, M.J.K. Bashir, The use of poly-aluminum chloride and alum for the treatment of partially stabilized leachate: A comparative study, Desalination 257 (2010) 110–116.
[15] A.A. Halim, H.A. Aziz, M.A.M. Johari, K.S. Ariffin, M.J.K. Bashir, Semi-aerobic landfill leachate treatment using carbon–minerals composite adsorbent, Environ. Eng. Sci. 29 (2012) 306–312.
[16] A. Bhatnagar, W. Hogland, M. Marques, M. Sillanpää, An overview of the modification methods of activated carbon for its water treatment applications, Chem. Eng. J. 219 (2013) 499–511.
[17] P. Xu, G.M. Zeng, D.L. Huang, C.L. Feng, S. Hu, M.H. Zhao, C. Lai, Z. Wei, C. Huang, G.X. Xie, Z.F. Liu, Use of iron oxide nanomaterials in wastewater treatment: A review, Sci. Total Environ. 424 (2012) 1–10.
[18] N.C. Feitoza, T.D. Gonçalves, J.J. Mesquita, J.S. Menegucci, M.-K.M.S. Santos, J.A. Chaker, R.B. Cunha, A.M.M. Medeiros, J.C. Rubim, M.H. Sousa, Fabrication of glycine-functionalized maghemite nanoparticles for magnetic removal of copper from wastewater, J. Hazard. Mater. 264 (2014) 153–160.
[19] APHA, WPCF, AWWA, Standard Methods for the Examination of Water and Wastewater, twenty-first ed., American Public Health Association (APHA), Washington, DC, 2005.
[20] K.Y. Foo, B.H. Hameed, Microwave-assisted preparation and adsorption performance of activated carbon from biodiesel industry solid reside: Influence of operational parameters, Bioresour. Technol. 103 (2012) 398–404.
[21] M.A. Bezerra, R.E. Santelli, E.P. Oliveira, L.S. Villar, L.A. Escaleira, Response surface methodology (RSM) as a tool for optimization in analytical chemistry, Talanta 76 (2008) 965–977.
[22] R. Droste, Theory and Practice of Water and Wastewater Treatment, Wiley & Sons, Hoboken, NJ, 1997.
[23] H. Alvarez-Vazquez, B. Jefferson, S.J. Judd, Membrane bioreactors vs conventional biological treatment of landfill leachate: A brief review, J. Chem. Tech. Biotechnol. 79 (2004) 1043–1049.
[24] S.L. Huo, B.D. Xi, H.C. Yu, L.S. He, S.L. Fan, H.L. Liu, Characteristics of dissolved organic matter (DOM) in leachate with different landfill ages, J. Environ. Sci. 20 (2008) 492–498.
[25] S.A. Al-Asheh, Z. Duvnjak, Sorption of cadmium and other heavy metals by pine bark, J. Hazard. Mater. 56 (1997) 35–51.
[26] X. Colom, F. Carrillo, F. Nogués, P. Garriga, Structural analysis of photodegraded wood by means of FTIR spectroscopy, Polym. Degrad. Stab. 80 (2003) 543–549.
[27] S. Naik, V.V. Goud, P.K. Rout, K. Jacobson, A.K. Dalai, Characterization of Canadian biomass for alternative renewable biofuel, Renewable Energy 35 (2010) 1624–1631.
[28] U. Garg, M.P. Kaur, G.K. Jawa, D. Sud, V.K. Garg, Removal of cadmium (II) from aqueous solutions by adsorption on agricultural waste biomass, J. Hazard. Mater. 154 (2008) 1149–1157.
[29] E. Pehlivan, B.H. Yanık, G. Ahmetli, M. Pehlivan, Equilibrium isotherm studies for the uptake of cadmium and lead ions onto sugar beet pulp, Bioresour. Technol. 99 (2008) 3520–3527.
[30] V. Gomez-Serrano, J. Pastor-Villegas, A. Perez-Florindo, C. Duran-Valle, C. Valenzuela- Calahorro, FT-IR study of rockrose and of char and activated carbon, J. Anal. Appl. Pyrolysis. 36 (1996) 71–80.
[31] A.C. Lua, T. Yang, Effect of activation temperature on the textural and chemical properties of potassium hydroxide activated carbon prepared from pistachio-nut shell, J. Colloid Interface Sci. 274 (2004) 594–601.
[32] R.G. Pearson, Hard and soft acids and bases, J. Am. Chem. Soc. 85 (1963) 3533–3539.
[33] A.R. Mohamed, M. Mohammadi, G.N. Darzi, Preparation of carbon molecular sieve from lignocellulosic biomass: A review, Renewable Sustainable Energy Rev. 14 (2010) 1591–1599.
[34] D. Adinata, W.M. Wandaud, M. Aroua, Preparation and characterization of activated carbon from palm shell by chemical activation with K_2CO_3, Bioresour. Technol. 98 (2007) 145–149.
[35] M. Chabani, A. Amrane, A. Bensmaili, Kinetics of nitrates adsorption on Amberlite IRA 400 resin, Desalination 206 (2007) 560–567.
[36] R.R. Sheha, A.A. El-Zahhar, Synthesis of some ferromagnetic composite resins and their metal removal characteristics in aqueous solutions, J. Hazard. Mater. 150 (2008) 795–803.
[37] S. Kushwaha, B. Sreedhar, P.P. Sudhakar, A spectroscopic study for understanding the speciation of Cr on palm shell based adsorbents and their application for the remediation of chrome plating effluents, Bioresour. Technol. 116 (2012) 15–23.
[38] S.L. Ching, M.Y. Yusoff, H.A. Aziz, M. Umar, Influence of impregnation ratio on coffee ground activated carbon as landfill leachate adsorbent for removal of total iron and orthophosphate, Desalination 279 (2011) 225–234.
[39] Z.M. Wu, Z.H. Cheng, W. Ma, Adsorption of Pb (II) from glucose solution on thiol-functionalized cellulosic biomass, Bioresour. Technol. 104 (2012) 807–809.
[40] M.H. Isa, L.S. Lang, F.A.H. Asaari, H.A. Aziz, N.A. Ramli, J.P.A. Dhas, Low cost removal of disperse dyes from aqueous solution using palm ash, Dyes Pigm. 74 (2007) 446–453.
[41] I.A.W. Tan, A. Ahmad, B. Hameed, Optimization of preparation conditions for activated carbons from coconut husk using response surface methodology, Chem. Eng. J. 137 (2008) 462–470.